Cd unit cell do indicate some tendency toward twofold symmetry, namely, space group *p*2.
31. We shall attempt to observe such enantiomorphism by epifluorescence microscopy. V. Von Tscharner and H. M. McConnel, *Biophys. J.* **36**, 409 (1981); M. Lösche and H. Möhwald, *Rev. Sci. Instrum.* **55**, 1968 (1984); G. B. Moore, C. M. Knobler, S. Akamatsu, F. Rondelez, *J. Phys. Chem.* **94**, 4588 (1990).
32. We thank C. Böhm and R. Kenn for assistance during the experiments, H. Möhwald for helpful discussions, A. Yonath for use of laboratory facilities at the Max Planck Unit for Structural Molecular Biology, and R. Feidenhans'l for help in the fitting analysis. Supported by the U.S.–Israel Binational Science Foundation, Jerusalem; the Petroleum Fund of the American Chemical Society; the German Israeli Foundation; the Fund for Basic Research of the Israel Academy of Science and Humanities; and the Danish Foundation for Natural Sciences. We thank Hasylab, DESY, Hamburg, for beam time.

2 November 1990; accepted 8 March 1991

Satellite Observations of Smoke from Oil Fires in Kuwait

S. S. Limaye, V. E. Suomi, C. Velden, G. Tripoli

Extensive dark smoke clouds associated with burning oil wells in Kuwait have been seen in data from weather satellites since early February 1991. The smoke is dispersed over a wide area. Variable and strong low level winds have held most of the smoke plume below 3 to 5 kilometers within a few hundred kilometers of the source. Thin veils of smoke have been detected in METEOSAT data as far away as 2000 kilometers east of Kuwait, over southwestern Pakistan at heights between 6 and 7 kilometers. The occasional presence of convective clouds over the fires indicates that some scavenging of the smoke is taking place.

Since early February 1991, extensive smoke clouds associated with burning oil wells in Kuwait have been seen in NOAA-10 and NOAA-11 polar orbiting satellite observations (*1*). Visible imagery from these and the METEOSAT geosynchronous satellite shows that the smoke plumes are quite dark (albedo generally <8%). At night the 0.84-μm channel on the polar satellites clearly shows a glow associated with the six isolated burning oil fields. The local impact of the smoke has been noted in media reports (*2*).

Before the ignition of the oil wells, several concerns were raised that the resulting smoke could have significant impact on climate by virtue of its ability to absorb sunlight over a large area (*3*). An essential element of these is that the smoke be lofted high in the atmosphere. A recent, more specific analysis of the fires in Kuwait suggests that the likely impacts on climate are small (*4*). The observations to date suggest that most of the smoke has been restricted to the lower atmosphere ($\leq$3 km) within ~1000 km of the source; however, some smoke has been detected at an altitude of 6 to 7 km nearly 2000 km from the source. Here we report on satellite observations of the dispersal of smoke from these fires over a larger region, estimates of the altitudes at which the smoke is detectable, and some interaction of the smoke with the transient synoptic weather patterns. As the regional weather is dynamic and seasonal, these observations should be viewed as illustrative, but provide an indication of the need for future monitoring.

Figure 1 shows the horizontal extent of the smoke as observed on 4 March 1991 in one solar (0.84 μm) and two infrared spectral bands (3.7 and 10.9 μm) from the NOAA-10 AVHRR sensor (*1*). The smoke cloud typically appears in the two short wavelength channels as dark plumes extending from four major fields in southern Kuwait (Fig. 1A) and from two fields north of Kuwait City (obscured by the high-level cirrus clouds in Fig. 1A). These sunlight-absorbing plumes were detectable over an area as much as 42,000 km^2, while the optically thicker region (optical thickness of about 2) blanketed an area as much as 7,100 km^2. On other days, relatively thin veils of smoke have been detected over a much larger area, nearly 180,000 km^2, such as on 18 March 1991. The coastline south of Kuwait City is completely obscured in the 0.6-μm channel (not shown) and can be seen just barely in the 0.84-μm data. Smoke plumes can be traced as light bands (lower brightness temperatures) to six clusters, the largest of which is south of Kuwait City [Burgan oil field, 210 wells (*4*)]. The average optical thickness of the smoke at 0.6 μm over the darkest parts is estimated to about 2, but varies with the ambient conditions and distance from the source. The smoke is typically detectable over the desert (high visible albedo) at optical thicknesses as low as about 0.2 from the visible data by its contrast and drift in time-lapse images but is not usually unambiguously detectable over water (low visible albedo) from satellite observations at either visible or infrared wavelengths.

The size of the particles and the heights to which they can rise are key factors that determine the extent of the areal spread, atmospheric residence times, and hence the degree of impact on weather or climate. The satellite observations present some information about both of these smoke characteristics. Small particles (comparable to the visible wavelengths) absorb sunlight but not the long wave thermal radiation emitted by the earth.

An indication of the average particle size is provided by the appearance of the smoke at different wavelengths. At visible wavelengths the smoke is dark; it is relatively transparent at 3.7 μm (Fig. 1B) and more so at 10.9 μm (Fig. 1C). The west shore of the Persian Gulf can be clearly seen at the longer wavelengths. These observations suggest that the smoke particles are predominantly smaller than about 1 μm, although some larger sized particles are also present, consistent with the expected size of the soot particles produced from oil fires (*5, 6*). However, the long wave transparency of the smoke within a few tens of kilometers of the source varies from day to day and also as a function of time of day. Satellite observations indicate that variations in the number density of the smoke particles and in the particle size distribution likely have resulted in variations (more larger particles) in the ambient atmospheric conditions and the amount of accompanying water vapor (because of the intrusion of water into the oil wells and as a combustion product and condensation onto the smoke particles). These are indicated by increased opacity at 3.7 and 10.9 μm, as well as by the appearance of water (white) clouds within the smoke plume in the visible images and supported by reports of black rain (*2*).

Height determination is the most difficult to achieve from satellite observations at visible wavelengths, but measurements of smoke drift, cloud shadows, and stereoscopic separation allow some estimates to be made. An indication of the relative level of the smoke plume is given by a few high-level clouds over the gulf that can be seen to cast shadows to the west onto the lower level smoke deck (Fig. 1A). The heights of small clouds over the smoke plume in the gulf region as estimated from their shadows are approximately 7 to 9 km. Nearby conventional upper air data (Shiraz, Iran) suggests that the clouds are at an approximate alti-

S. S. Limaye, V. E. Suomi, C. Velden, Space Science and Engineering Center, University of Wisconsin–Madison, 1225 West Dayton Street, Madison, WI 53706.
G. Tripoli, Department of Meteorology, University of Wisconsin–Madison, Madison, WI 53706.

tude of 9.5 km, so that the altitude of the smoke plume over the gulf was no more than about 0.5 to 2.5 km on this particular day at sunrise. No shadows of the smoke plumes themselves have yet been identified, which also suggests that the plumes are not higher than about 3 km within a distance of about 50 km from the source.

Although the spatial resolution of the geostationary satellite observations (METEOSAT and INSAT) is lower than that of the polar satellites, their continuous imagery is particularly useful in monitoring the movement of the smoke which, coupled with the knowledge of winds from weather forecast models provides another estimate of the heights to which smoke has risen. On 8 March 1991, the smoke could be tracked as far as 2000 km east of the source region (Fig. 2) in visible METEOSAT images. Measurements made from several such images acquired around 12:00 UT showed that smoke cloud drift speeds exceeded 25 m s^{-1}. Comparison with the National Meteorological Center (NMC) global analysis of the upper level observations showed that the level of the smoke cloud had to have been between 400 and 500 mbar (6 to 7 km above the surface). It has been generally easier to detect the smoke drift over land in time-lapse displays of the imagery than it is to make quantitative measurements of its optical thickness, drift, and altitude because the smoke optical thickness is not very high at several hundred kilometers from the source. So far the smoke has not been discerned in the METEOSAT water vapor channel (which is sensitive to the mid-troposphere water vapor). These data either indicate that very low amounts of water vapor are associated with the smoke plume, or, more likely, that the plume is restricted to the lower atmosphere, or both.

The heights to which smoke can rise depends on the strength of the heat source. The 3.7-μm AVHRR data clearly pinpoint the hot spots, which are averaged over each pixel (roughly 1.1 by 1.1 km) and have brightness temperatures between 310 and 320 K as the source of the smoke (Fig. 1B). A large difference in brightness temperatures

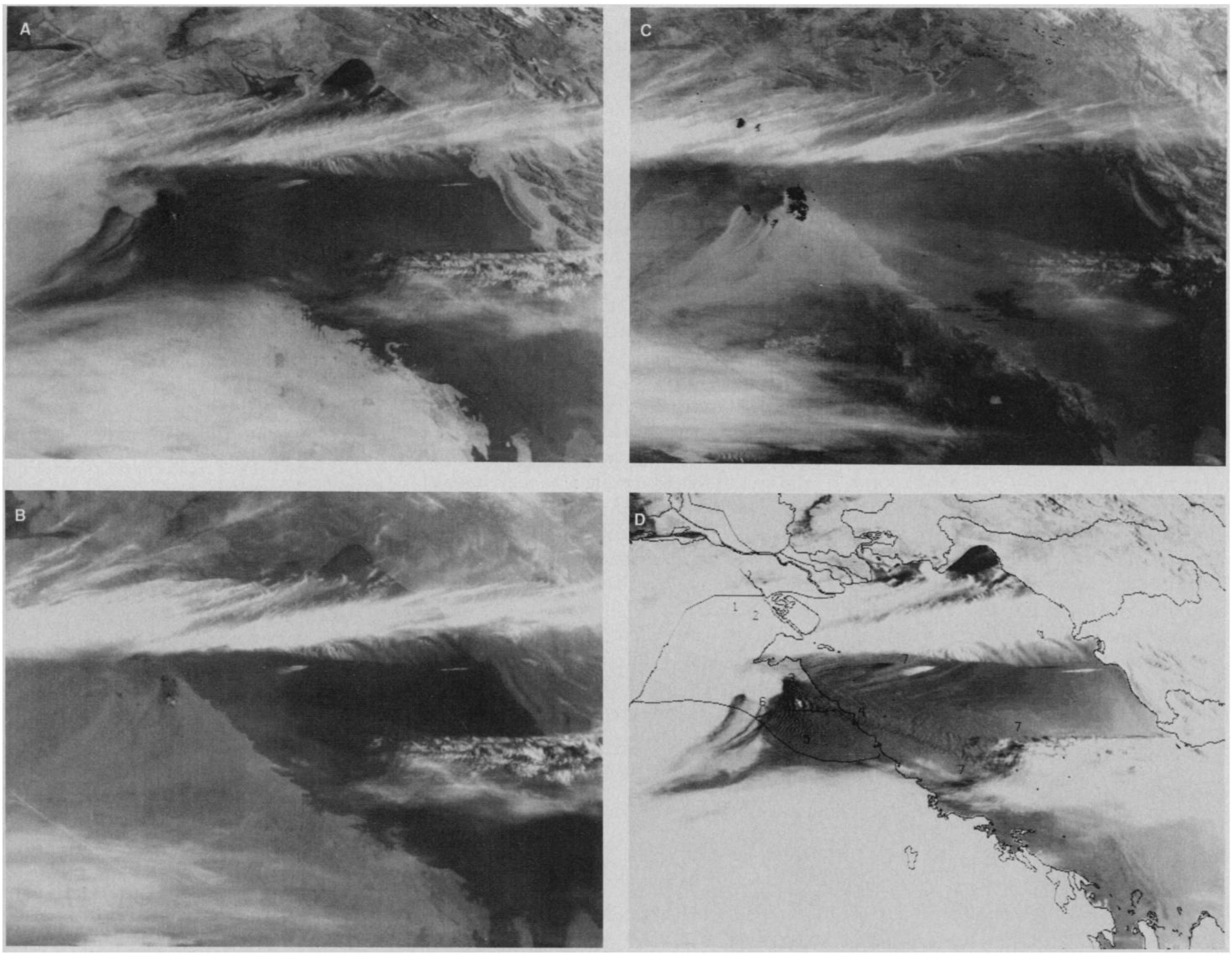

Fig. 1. A section of the NOAA-10 Advanced Visible High Resolution Radiometer observations recorded on 4 March 1991 beginning at 4:23:00 UT in Channel 1 (0.58 to 0.68 μm) (**A**), Channel 3 (3.55 to 3.93 μm) (**B**), and Channel 4 (10.3 to 11.3 μm) (**C**). The smoke appears dark in the shortwave channel (A) and light in the infrared channels (B and C). The brightness scale for (B) and (C) is such that high radiances are depicted as black and low radiances as white. The smoke plume can be seen extending westward near the surface and to the southeast over the Persian Gulf, as far as Bahrain (lower right) at slightly higher levels. A convective cloud is also seen at thesoutheast source region that appears responsible for the train of gravity waves extending over the Persian Gulf (A). Numerous black dots in (B) indicate the presence of hot spots due to gas flares at refineries and other industrial facilities. (D) shows the geographic area covered and identifies the major oil fields (Rawdatayn, 1; Sabiriyah, 2; Ahmadi, 3; Burgan, 5; Umm Gudair, 6; and Mina Saud refinery, 4) and several cloud shadows used for estimating plume height (7). The base image is a contrast stretched version of (A) that shows the gravity waves. The political outlines are given for reference.

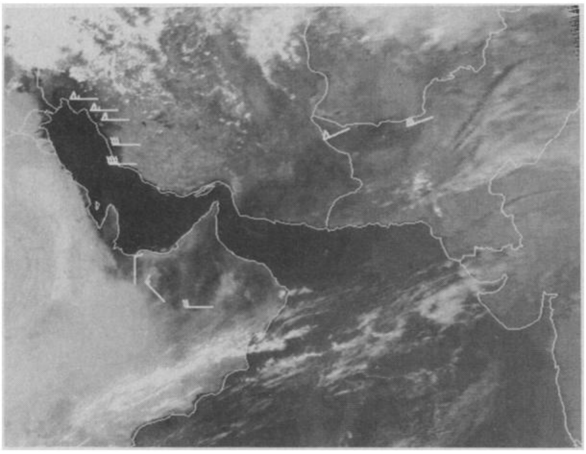

Fig. 2. A section of METEOSAT visible image acquired on 8 March 1991 at 11:30 UT. Smoke is seen extending from the source along Persian Gulf and northwards over the Arabian sea and into Western Pakistan. The wind barbs indicate the measured drift rate of the smoke for illustration. The measured speed and direction suggest that the smoke is between 500- and 400-mbar pressure level or between 6 and 7 km altitude on the basis of the NMC global analysis.

at 3.7 and 10.9 μm indicates that the emission area is only a small fraction of the spatial resolution of the data (*7*). While, in principle, it would be possible to estimate the total energy output from the oil fires, there is evidence that the 3.7-μm data covering approximately 120 km^2 is saturated and thus an estimate of the oil burning rate is precluded. Nevertheless there are reports that between 1.5 and 6 million barrels are being burnt per day (*2, 4*), amounting to a heat injection into the atmosphere of between approximately 1.5×10^{11} and 6.0×10^{11}.

Such an intense heat source is able to cause convection under the right conditions. Convective clouds over the oil fires can often be seen in the satellite data. One such event can be seen in Fig. 1, where a cloud was generated over the Burgan oil field in southeastern Kuwait; gravity waves of approximately 6-km wavelength emanated from the cloud and propagated southeastward for a considerable distance (Fig. 1D). The persistence of these waves suggests that they were vertically trapped within the cool low-level air mass and that this air mass was not reaching the upper parts of the atmosphere.

The generation of convective clouds indicates that at least some of the smoke is being scavenged. The scavenging was studied with a three-dimensional computer simulation of fire plumes forced by the Kuwait oil fires; average April 1990 conditions and a triply nested model were used (*9*). The results showed that for the relatively moist conditions in April, more than 98% of the emitted smoke would be scavenged within 6.5 km of the ground in a cumulus cloud formed by the warm smoke plume. The assumed conditions were, however, exceptionally conducive to moist convection because of high humidity and relatively cool upper air temperatures. Several examples of local deep convection forced by the fires have already been observed. Figure 3 shows one such example from 15 March 1991. The absence of a visible smoke plume moving away from the fires in this image suggests that much of the smoke is indeed removed locally or regionally. Smoke-triggered convection, however, has been relatively rare; most of the scavenging has likely been due to transient systems.

The primary effect of the smoke is to block sunlight while allowing long wave radiation to escape. Thus the diurnal cycle of surface temperatures under the smoke canopy and away from the immediate environment of the source would be suppressed. The smoke cloud thus restricts heating of the underlying surface during the day while allowing the surface to cool at night because its infrared absorption cross section is small (*6*). Lower than normal surface temperatures have been reported in the media (*2*) during cloudless but smoky daylight periods. The emission from the warm smoke plume and its opacity appear to prevent unambiguous detection of the lowered surface temperatures from satellite data (*8*). The upper portions of the smoke plume absorb sunlight and heat the atmosphere above the surface. As a result, during the day an inversion layer is expected to form under the smoke canopy with the denser colder air trapped near the surface and warmer air within the sun-heated smoke. Disruption of this stable situation by interaction with invading air masses on a synoptic scale is a major factor in the dispersal of the smoke both horizontally and vertically and thus determines the severity of the local and regional air pollution. As far as 1100 km away from the source the smoke optical thickness has been observed to be high enough to obscure the ground in isolated pockets several hundred square kilometers large. More systematic observations are needed to study the extent of regional impact.

REFERENCES AND NOTES

1. Two visible channels centered at approximately 0.6 and 0.9 μm and two infrared channels at 3.7 and 10.9 μm provide observations at 1.1-km spatial resolution at nadir (NOAA-11 AVHRR has an additional infrared channel at 11.5 μm). Placed in sun-synchronous polar orbits, NOAA-10 provides coverage at roughly local 0600 and 1800 hours whereas NOAA-11 provides coverage at approximately local noon and midnight.
2. E. Schmitt, *New York Times*, 3 March 1990, p. 13; D. Lorch, *ibid*. 6 March 1991, p. 1; Cable News Network (CNN), 10 March 1991; R. Tyson and S. V. Meddis, *USA Today*, 15 to 17 March 1991; and CNN Prime Time News, 18 March 1991 reported that visibility was only about 500 m because of smoke blown over Kuwait City from the oil fields and daytime temperature of 15°C on an otherwise cloudless day. On this day the smoke could be seen to drift over the desert along the Persian Gulf coast for a distance of nearly 1200 km before turning eastward toward the northern Arabian Sea. Over this entire distance the east-west extent of the plume was less than 150 km. Routine weather observations from Kuwait City are not yet available; those from other stations in the region are also not available through the normal channels. Some in situ measurements of the smoke have been made by flights through the smoke (M. Simons, *New York Times*, 16 April 1991, p. B7) and more are planned.
3. P. Aldous, *Nature* **349**, 96 (1991).
4. R. D. Small, *ibid*. **350**, 11 (1991).
5. A. B. Pittock *et al*., *SCOPE 28, Environmental Consequences of Nuclear War*, vol. 1, *Physical and Atmospheric Effects* (International Council of Scientific Unions; Wiley, New York, ed. 2, 1989).
6. R. P. Turco, O. B. Toon, T. P. Ackerman, J. B. Pollack, C. Sagan, *Science* **247**, 166 (1990).

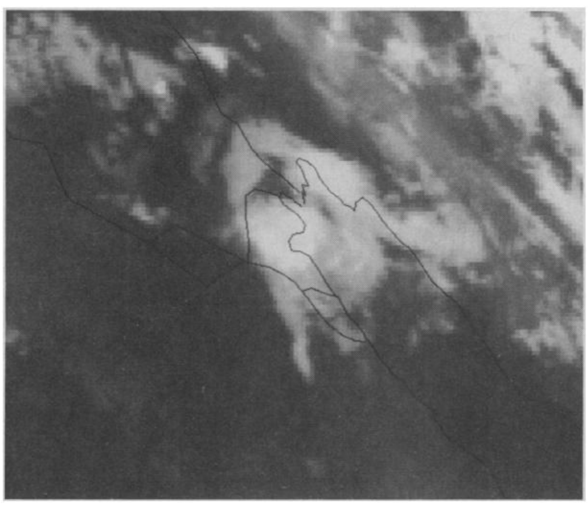

Fig. 3. A dramatic illustration of a convective cloud believed to be associated with the oil field fires as observed on 15 March 1991 in METEOSAT visible and infrared observations. This infrared window channel image was acquired beginning at 17:30 UT. The circular annulus seen around the bright cloud mass centered roughly over Kuwait City was observed throughout the afternoon.

7. M. Matson and J. Dozier, *Photogramm. Eng. Rem. Sensing* 47, 1311 (1981).
8. There are few weather observations available at present in this region at this time. Even the temperature sounding capability from the polar satellites may be somewhat suspect until the impact of the enhanced CO_2 abundances within the plume and the effects of smoke opacity are better known.
9. G. J. Tripoli, in preparation. The model used a triply nested grid with 1.5-, 4.5-, and 13.5-km resolutions. Fires were represented by a mean heat and smoke flux into a cylindrical region 750 m deep and 10 km in diameter; the heat source was taken to be 8.6 kWm^{-2}, a worst case estimate. It was also assumed that 100% of the smoke would be activated as cloud droplet nuclei in the event that air saturation was reached and that scavenging would occur if the smoke containing cloud droplets were collected onto a falling precipitation particle. The mean April winds used for the simulation were relatively strong, reaching 45 m s^{-1} at upper levels. The observed convective cloud system seen in Fig. 3 similarly developed in a conditionally unstable environment as the sun rose in the sky and a low-level pressure trough could be seen traversing over the area. While the ambient upper level flow from the northwest could be clearly seen, the cloud was seen to grow over the fires in late afternoon and eventually emit a circular ring as seen in this late-stage image.
10. The METEOSAT and NOAA-10 digital data were received at the Space Science and Engineering Center of the University of Wisconsin–Madison. Cooperation of many individuals in gathering and analysis of these data is gratefully acknowledged. Discussions with F. Bretherton, D. W. Martin, L. A. Sromovsky, J. Kutzbach, and H. S. Limaye have been particularly useful. Finally, we thank two anonymous referees for their comments.

21 March 1991; accepted 1 May 1991

$^{40}Ar/^{39}Ar$ Age of Cretaceous-Tertiary Boundary Tektites from Haiti

G. A. Izett, G. B. Dalrymple, L. W. Snee

$^{40}Ar/^{39}Ar$ dating of tektites discovered recently in Cretaceous-Tertiary (K-T) boundary marine sedimentary rocks on Haiti indicates that the K-T boundary and impact event are coeval at 64.5 ± 0.1 million years ago. Sanidine from a bentonite that lies directly above the K-T boundary in continental, coal-bearing, sedimentary rocks of Montana was also dated and has a $^{40}Ar/^{39}Ar$ age of 64.6 ± 0.2 million years ago, which is indistinguishable statistically from the age of the tektites.

The discovery of relic tektites (*1, 2*) in K-T boundary rocks near Beloc, Haiti, has opened the door for geochemical studies needed for an understanding of K-T boundary phenomena, including the isotopic dating of these unusual objects. Tektites are glass-melt droplets formed by the instantaneous fusion of terrestrial rocks during large-scale hypervelocity impact events (*3*). The Haitian tektites are similar in composition and morphology to other classes of tektites (*1*), but their stratigraphic position and our new isotopic ages show that they are nearly twice as old as North American tektites [35.4 and 35.5 million years ago (Ma)], which were the oldest tektites known (*4*).

For the past 30 years, the goal of numerous isotopic studies has been to obtain an accurate age for the K-T boundary. This goal assumed new importance after an Ir anomaly (*5*) and shock-metamorphosed quartz grains were discovered (*6*) in K-T boundary rocks worldwide, indicating that one, or possibly several, large asteroids or comets struck Earth at the end of the Cretaceous Period. Particular efforts have been made to date minerals in bentonite (altered volcanic ash) beds that occur in coal-bearing nonmarine sedimentary rocks 1 to 21 m above the K-T boundary in western North America (*7–9*). These studies have established ages that range from 63.5 to 66.0 Ma for nonmarine rocks, but the isotopic age of marine rocks, which also record the K-T impact event at numerous sites worldwide (*5, 6*), had not been determined. To fill this gap in knowledge, we report $^{40}Ar/^{39}Ar$ ages for the Haitian tektites and, for control and correlation, for sanidine crystals from nonmarine bentonite (HC bentonite) in the Z coal bed that lies directly above the K-T boundary in the Hell Creek area of Montana (*9*).

The Haitian tektites occur together with an Ir abundance anomaly (2.3 ppb) and shock-metamorphosed quartz grains in a marl bed 0.5 m thick that marks the paleontologic K-T boundary (*1, 10*). This marl bed is in the lower part of the Beloc Formation, a sequence 150 m thick of marine limestone (*11*).

A remarkable feature of this bed is its content of numerous clay pellets, and about 2% of the pellets in the lower 2 cm of the bed contain relic tektites (*1*). The pellets occur throughout the bed, but they are most abundant (~60%) near its base (*1*). A typical tektite-bearing clay pellet consists of a corroded glass core enclosed within a jacket or shell of iron-rich smectite. The smectite shell is the alteration product of the glass. Many pellets are hollow and others are solid. About 75% have irregular, rounded shapes, but the remaining 25% have shapes typical of tektites (*12*), including spheroids, discoids, spindles, teardrops, rods, and dumbbells. Spherical pellets vary from 0.5 to 3.5 mm in diameter; dumbbells, teardrops, spindles, and irregular-shaped objects range from 3 to 10 mm in length. In 1980, these pellets were referred to as possible microtektites by Maurrasse (*13*) and 10 years later as altered tektites by Hildebrand and Boynton (*10*).

In reflected light, most tektites are dark brown to black, but in transmitted light they range from pale brown to pale yellowish brown (Fig. 1). Rare tektites have a golden honey color. Some contain spherical (common) and almond-shaped (less common) bubbles, but all lack microlites and crystallites characteristically found in volcanic glass such as obsidian. The presence of glass in the smectite pellets, some of which have shapes identical to tektites, confirms that they are pseudomorphs of tektites (*1*). We refer below to the glass cores simply as tektites.

The major element chemical composition of the Haitian tektites (*1, 2*) is broadly similar to that of other tektite groups (*4*), except that the Haitian tektites have lower SiO_2 content (mean, 64%; range, 52 to 68%) and higher Fe, Ca, and Na contents. The K content of the tektites is adequate for $^{40}Ar/^{39}Ar$ dating (average, 1.2%; range, 0.7 to 1.5%).

The honey-colored tektites have extraordinarily high amounts of Ca and S (25% CaO and 0.4% S) for natural glasses (*14*). The high content of these elements suggests that some of the target materials melted during the K-T impact may have been marine rocks rich in $CaSO_4$. Beds of anhydrite have been identified in the subsurface at a candidate impact site (Chicxulub) on the Yucatan platform (*15, 16*). The anomalously high content of S and the S isotopic com-

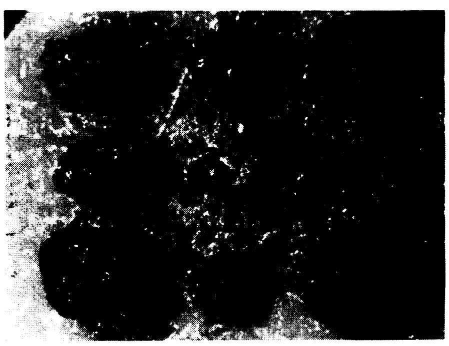

Fig. 1. Remnant glass cores of ten tektites from the K-T boundary marker bed on Haiti showing typical corroded surfaces. Some smectite remains on the sulfur-rich tektite near the center. The tektite in the lower right corner 1.8 mm long.

G. A. Izett and L. W. Snee, U.S. Geological Survey, Mail Stop 913, Denver Federal Center, Denver, CO 80225.
G. B. Dalrymple, U.S. Geological Survey, Mail Stop 937, 345 Middlefield Road, Menlo Park, CA 94025.